JOURNAL OF AGRICULTURAL AND FOOD CHEMISTRY

Agricultural and Environmental Chemistry

Structure-based Virtual Screening, Compound Synthesis and Bioassay for the Design of Chitinase Inhibitors

Yawen Dong, Xi Jiang, Tian Liu, Yun Ling, Qing Yang, Li Zhang, and Xiongkui He

J. Agric. Food Chem., **Just Accepted Manuscript** • DOI: 10.1021/acs.jafc.8b00017 • Publication Date (Web): 20 Mar 2018

ACS Publications

is published by the American Chemical Society. 1155 Sixteenth Street N.W., Washington, DC 20036

1 **Structure-based Virtual Screening, Compound Synthesis and Bioassay for the Design of**

2 **Chitinase Inhibitors**

3 Yawen Dong,[†] Xi Jiang,[‡] Tian Liu,[‡] Yun Ling,[†] Qing Yang,*[,‡] Li Zhang,*[,†] and Xiongkui He[†]

4 [†] Department of Applied Chemistry, College of Science, China Agricultural University, Beijing

5 100193, China.

6 [‡] State Key Laboratory of Fine Chemicals and School of Life Science and Biotechnology, Dalian

7 University of Technology, Dalian 116024, China.

8

9 *Corresponding Author:

10 Dr. Li Zhang,

11 Tel: +86-010-6273-0345

12 Fax: +86-010-6273-0345

13 E-mail: zhang_li@cau.edu.cn

14 Prof. Qing Yang,

15 Tel: +86-411-8470-7245

16 Fax: +86-411-8470-7245

17 E-mail: qingyang@dlut.edu.cn

18

ABSTRACT

Chitinases play a vital part in the molting phase of insect pests. Inhibiting their activities by the use of drug-like small chemical molecules is thought to be an efficient strategy in pesticide design and development. Based on the crystal structure of *Of*ChtI, a chitinase indispensable for molting of the insect pest *Ostrinia furnacalis* (Asian corn borer), here we report a chemical fragment and five variant compounds as inhibitors of *Of*ChtI obtained from a library of over 200,000 chemicals by a structure-based virtual screening approach. The compounds were synthesized with high atom economy and tested for their *Of*ChtI inhibitory activities in a bioassay. Compound **3** showed preferential inhibitory activity with a K_i value of 1.5 μM against *Of*ChtI. Analysis of the structure-activity relationships of the compounds provided insight into their interactions with the enzyme active site, which may inform future work to improve the potency of the inhibitory activity.

KEYWORDS: chitinase, inhibitors, fragment, structure-based virtual screening, structure-activity relationship

33 **INTRODUCTION**

34 Chitin, a long-chain polymer composed of β-1,4 linked *N*-acetyl-D-glucosamine (GlcNAc), is a
35 vital structural component of insects.[1] As well as being important for insect growth and development,
36 it also supports the integrity of the cuticle that is secreted by the epidermal cells. The cuticle takes the
37 shape of the exoskeleton and has only a limited ability to expand as the insect grows, so it undergoes
38 periodic degradation to allow molting, and is then re-synthesized as part of the new exoskeleton that
39 is formed after molting has occurred.[2] Solid state NMR spectroscopy has shown that the composition
40 of chitin differs considerably between different types of insect cuticles, and that it can make up to 40%
41 of the exuvial dry mass depending upon the insect species.[3] Given the obvious importance of chitin
42 as a structural component of insects, there is much interest in understanding whether and how its
43 activity or production could be inhibited as a novel approach to the control of insect pests.

44 During the molting stage of insects, the glycoside hydrolase family 18 (GH18) chitinases (EC
45 3.2.1.14),[4,5] that are secreted from epithelial cells, are key enzymes that catalyze the hydrolysis of
46 chitinous components of the old cuticle into constituent oligosaccharides.[6,7] It is clear that if the
47 activities of GH18 chitinases were blocked by small molecule inhibitors, the molting process would
48 be disrupted and growth and development would not continue in the normal way, possibly even
49 resulting in death. Thus, small molecule chitinase inhibitors represent promising candidates for the
50 design and development of novel pesticides for the control of insect pests.[8-13]

51 Several known GH18 chitinase inhibitors have already been described in the literatures; some of
52 these are natural products, such as allosamidin,[14-16] argifin,[17] argadin,[18] cyclo-(L-Arg-D-Pro),[19]
53 psammaplin,[20] styloguanidine,[21] and $(GlcN)_5$;[22] others are chemically manufactured, such as

54 pentoxifylline and its analogs,[23] and biodionin B and its derivatives.[24] However, whilst such chitinase
55 inhibitors have been reported, their widespread use is impeded by the fact that they are difficult to be
56 synthesized and their effects can be relatively weak. Thus, researches need to be carried out to
57 identify more potent and easily synthesizable inhibitors of chitinase.

58 Recently, structure-based virtual screening (SBVS) and fragment-based drug discovery have been
59 rapidly developed as e□ective methods to identify hits.[25-28] Having characterized the crystal
60 structures of chitinase as well as the co-crystal structures of enzyme-inhibitor complexes, the
61 structure-activity relationships have been revealed, and SBVS has been used to identify potential
62 chitinase inhibitors.[29-31] A typical GH18 chitinase usually possesses a long cleft-like catalytic domain
63 with multiple binding subsites labelled by +2, +1, -1, -2, -3, -4, and -5, respectively, and catalysis
64 always occurs between the subsites +1 and -1.[32] Not surprisingly, chitinase structural biology studies
65 have offered valuable opportunities in the rational design of new and bio-available inhibitors via *in*
66 *silico* analysis.[33]

67 A chitinase of GH18 from the agricultural pest *Ostrinia furnacalis* (Asian corn borer), *Of*ChtI,
68 plays a critical role in the degradation of old cuticle during the molting stage, and is deemed to be a
69 potential target for the development of effective chitinase inhibitors. To date, there have been few
70 reports of *Of*ChtI inhibitors. They are known to have complex structures.[22,30,34] In this study, we
71 utilized the reported crystal structure of the chitinase *Of*ChtI with its bound ligand, $(GlcNAc)_3$,[35] to
72 obtain inhibitors with high potency and that are easy to synthesize. Using a combination of SBVS
73 and biological evaluation, we sought to obtain a fragment of
74 2-amino-6-methyl-4,5,6,7-tetrahydro-benzo[*b*]thiophene-3-carboxylic acid ethyl ester, from which to

75 develop potent inhibitors against *Of*ChtI. The synthetic route used in the synthesis of the inhibitor
76 compound facilitated an atom-economic means of designing the final compound, which would
77 improve the sustainability of its manufacture on a larger scale.
78

79 **MATERIALS AND METHODS**

80 **Chemical Database Preparation**. The chemical database SPECS,[36] a library of 200,000 single
81 synthesized well-characterized small molecules, was used for structure-based virtual screening in
82 order to identify potential candidate compounds. The descriptors of all the screened molecules, such
83 as their molecular weight (MW), octanol-water partition coefficient (Clog P), number of rotatable
84 bonds (ROB), number of aromatic bonds (ARB), number of H-bond acceptors (HBA), and number
85 of H-bond donors (HBD), were calculated by the Descriptors Program of Molecular Operating
86 Environment drug discovery modelling software (MOE 2016.08).[37] The molecules were then
87 evaluated according to whether they fulfilled certain 'pesticide-likeness' parameters, as defined by
88 Gefei Hao *et al.*,[38] and those that did not meet the criteria were filtered out of the database.

89 **Pharmacophore-based Screening**. Pharmacophore-based screening was carried out using the
90 Virtual Screening program of MOE modelling software (MOE 2016.08). Two crystal structures of
91 *Of*ChtI with the bound ligands were downloaded from the RCSB Protein Data Bank (PDB ID: 3WL1
92 and 3WQV),[35] and were used to establish a well-tested pharmacophore model. On the basis of the
93 alignment and superposition of the two crystal structures, the spatial positioning and interactions
94 between receptor and ligand were analyzed carefully and the common features, such as the
95 hydrophobic center and hydrogen bond acceptor and donor, were set as pharmacophore features.

96 These features were then used to screen the dataset of molecular candidates obtained from the
97 SPECS database. Molecules not containing the defined pharmacophore features were screened out of
98 the dataset.

99 **Molecular Docking.** Molecular docking was employed in order to generate elementary prediction
100 of the binding modes and energies between the protein (*Of*ChtI) and the candidate molecules. The
101 co-crystal structure of *Of*ChtI with its bound ligand $(GlcNAc)_3$ (PDB ID: 3WL1) was used as a
102 template for the molecular docking. To prepare the protein structure, the Structure Preparation
103 function in MOE was used. The process included assessing the quality of the protein structure data
104 using defined temperature factors, protein geometry checks and electron density checks, adding
105 hydrogen atoms and optimizing their positions, and performing final energy minimization of the
106 structure. Following this, molecular docking was performed by the Dock application of MOE, with
107 two rounds of calculation. A collection of poses were generated from the pool of ligand
108 conformations using the Triangle Matcher method, and were further refined using the Rigid Receptor
109 method in MOE. Finally, a generalized Born/volume integral implicit solvent model, GBVI/WSA dG,
110 developed by Labute[39] was used for scoring each of the generated poses, and for each compound the
111 pose with the lowest score was retained. Compounds were then ranked low to high based on the
112 scores.

113 **Cluster Analysis.** In order to categorize the compounds obtained by molecular docking on the
114 basis of their structural diversity, the SAReport program in MOE was used in accordance with the
115 method presented by Alex.[40] A grid of molecule fragments was constructed to reveal common
116 molecular scaffold classes and statistics on the number of matched molecules, number of heavy

117 atoms and maximum similarity to any already picked molecular scaffold were calculated.

118 **Chemicals and Instruments.** All laboratory reagents were acquired from Ouhe Corporation
119 (Beijing, China) and were of analytical grade. The target compounds were purified by column
120 chromatography on silica gel 60, 200-300 mesh (Puke Corporation, Qingdao, China). Melting points
121 of the compounds were measured using an X-4 binocular microscope (Fukai Corporation, Beijing,
122 China) with uncorrected values. The ^{1}H NMR and ^{13}C NMR spectra of the purified target compounds
123 were determined by an AM-300 spectrometer (Bruker, Bremen, Germany) at 300 MHz for ^{1}H and 75
124 MHz for ^{13}C, respectively. Deuteriochloroform ($CDCl_3$) or DMSO-d_6 was used as the solvent and
125 tetramethylsilane (TMS) was used as the internal standard. High resolution mass spectrometry
126 (HRMS) data were obtained on a 7.0T FTICR-MS instrument (Varian, Palo Alto, CA).

127 **General Procedure for the Synthesis of the Precursors 2a-5a and 1**. As shown in Figure 1, the
128 elemental sulfur (1 equiv.) was added into the mixture of substituted cyclohexanone (1 equiv.) and
129 cyano compound (1 equiv.) in ethanol. Then the morpholine (1 equiv.) was added dropwise as a base
130 of catalyst. The reaction mixture was stirred at 85 □ for about 5 h. After that, the solvent was
131 evaporated and the residue was dissolved in ethyl acetate. The organic layer was washed with water,
132 dried with anhydrous sodium sulfate, filtered and evaporated for purification.

133 2-Amino-5-methyl-4,5,6,7-tetrahydro-benzo[*b*]thiophene-3-carboxylic acid ethyl ester (**2a**) was
134 synthesized in line with the general procedure with 3-methylcyclohexanone (1 g, 8.9 mmol), ethyl
135 cyanoacetate (1.007 g, 8.9 mmol) and elemental sulfur (0.285 g, 8.9 mmol) in ethanol (8 mL). The
136 crude product was purified with column chromatography on silica gel (Petroleumether ether/ethyl

137 acetate = 10:1, v/v). White solid; yield 89.12%; mp: 70-71 □; ^{1}H NMR (300 MHz, $CDCl_3$) δ 5.94 (s,
138 2H), 4.26 (q, *J* = 7.1 Hz, 2H), 2.99-2.84 (m, 1H), 2.66-2.34 (m, 2H), 2.27-2.09 (m, 1H), 1.90-1.68 (m,
139 2H), 1.46-1.27 (m, 1H), 1.33 (t, *J* = 7.1 Hz, 3H), 1.04 (d, *J* = 6.6 Hz, 3H).

140 2-Amino-6-methyl-4,5,6,7-tetrahydro-benzo[*b*]thiophene-3-carboxylic acid propyl ester (**3a**) was
141 synthesized in line with the general procedure with 4-methylcyclohexanone (0.5 g, 4.5 mmol), propyl
142 cyanoacetate (0.572 g, 4.5 mmol) and elemental sulfur (0.144 g, 4.5 mmol) in ethanol (5 mL). The
143 crude product was purified with column chromatography on silica gel (Petroleumether ether/ethyl
144 acetate = 10:1, v/v). White solid; yield 82.80%; mp: 62-63 □; ^{1}H NMR (300 MHz, $CDCl_3$) δ 7.21 (s,
145 2H), 4.06 (t, *J* = 6.5 Hz, 2H), 2.77 (d, *J* = 16.9 Hz, 1H), 2.59-2.39 (m, 2H), 2.12-1.96 (m, 1H),
146 1.84-1.71 (m, 2H), 1.71-1.55 (m, 2H), 1.36-1.16 (m, 1H), 0.98 (d, *J* = 6.5 Hz, 3H), 0.93 (t, *J* = 7.4 Hz,
147 3H).

148 2-Amino-6-tert-butyl-4,5,6,7-tetrahydro-benzo[*b*]thiophene-3-carboxylic acid ethyl ester (**4a**) was
149 synthesized in line with the general procedure with 4-tert-butylcyclohexanone (1 g, 6.5 mmol), ethyl
150 cyanoacetate (0.735 g, 6.5 mmol) and elemental sulfur (0.208 g, 6.5 mmol) in ethanol (10 mL). The
151 crude product was purified with column chromatography on silica gel (Petroleumether ether/ethyl
152 acetate = 30:1, v/v). Yellow liquid; yield 85.70%; ^{1}H NMR (300 MHz, $CDCl_3$) δ 5.93 (s, 2H), 4.25 (q,
153 *J* = 7.1 Hz, 2H), 3.04-2.89 (m, 1H), 2.58-2.41 (m, 2H), 2.35-2.21 (m, 1H), 2.02-1.88 (m, 1H),
154 1.53-1.39 (m, 1H), 1.33 (t, *J* = 7.1 Hz, 3H), 1.30-1.18 (m, 1H), 0.91 (s, 9H).

155 2-Amino-6-methyl-4,5,6,7-tetrahydro-benzo[*b*]thiophene-3-carboxylic acid isopropyl ester (**5a**)
156 was synthesized in line with the general procedure with 4-methylcyclohexanone (1.000 g, 8.9 mmol),

157 isopropyl cyanoacetate (1.134 g, 8.9 mmol) and elemental sulfur (0.286 g, 8.9 mmol) in ethanol (10
158 mL). The crude product was purified with column chromatography on silica gel (Petroleumether
159 ether/ethyl acetate = 50:3, v/v). Yellow solid; yield 86.68%; mp: 67-68 □; ^{1}H NMR (300 MHz,
160 $CDCl_3$) δ 5.89 (s, 2H), 5.31-5.04 (m, 1H), 2.94-2.79 (m, 1H), 2.68-2.48 (m, 2H), 2.19-2.01 (m, 1H),
161 1.94-1.76 (m, 2H), 1.42-1.21 (m, 1H), 1.32 (d, J = 2.9 Hz, 3H), 1.30 (d, J = 2.9 Hz, 3H), 1.04 (d, J =
162 6.5 Hz, 3H).

163 2-Amino-6-methyl-4,5,6,7-tetrahydro-benzo[*b*]thiophene-3-carboxylic acid ethyl ester (**1**) was
164 synthesized in line with the general procedure with 4-methylcyclohexanone (1 g, 8.9 mmol), ethyl
165 cyanoacetate (1.009 g, 8.9 mmol) and elemental sulfur (0.286 g, 8.9 mmol) in ethanol (10 mL). The
166 crude product was purified with column chromatography on silica gel (Petroleumether ether/ethyl
167 acetate = 50:1, v/v). Yellow solid; yield 86.98%; mp: 106-107 □; ^{1}H NMR (300 MHz, DMSO-d_6) δ
168 7.19 (s, 2H), 4.13 (q, J = 7.1 Hz, 2H), 2.75 (d, J = 17.3 Hz, 1H), 2.56-2.29 (m, 2H), 2.13-1.88 (m,
169 1H), 1.82-1.51 (m, 2H), 1.37-1.10 (m, 1H), 1.23 (t, J = 7.1 Hz, 3H), 0.97 (d, J = 6.5 Hz, 3H). ^{13}C
170 NMR (75 MHz, DMSO-d_6) δ 165.11, 163.07, 130.98, 115.03, 102.63, 58.62, 32.12, 30.73, 29.01,
171 26.32, 21.30, 14.40.

172 **General Procedure for the Synthesis of the Target Compounds 2-6**. As shown in Figure 1, the
173 acyl chloride (1.1 equiv.) was added dropwise in the mixture of the precursor (1 equiv.) and TEA (1.2
174 equiv.) in dichloromethane at 0 □. The reaction mixture was stirred overnight at room temperature.
175 After that, the organic layer was washed with 1 mol/L HCl solution, saturated sodium bicarbonate
176 solution and water, dried with anhydrous sodium sulfate, filtered and evaporated for purification.

2-(3,4-Dimethoxybenzamido)-5-methyl-4,5,6,7-tetrahydro-benzo[*b*]thiophene-3-carboxylate acid ethyl ester (**2**) was synthesized in line with the general procedure with compound **2a** (0.7 g, 2.9 mmol) and 3,4-dimethoxybenzoyl chloride (0.64 g, 3.2 mmol). The crude product was purified with crystallization from ethyl acetate. White solid; yield 87.0%; mp: 114-115 □; ^{1}H NMR (300 MHz, $CDCl_3$) δ 12.26 (s, 1H), 7.62 (d, *J* = 2.0 Hz, 1H), 7.55 (dd, *J* = 8.4, 2.0 Hz, 1H), 6.94 (d, *J* = 8.4 Hz, 1H), 4.37 (q, *J* = 7.1 Hz, 2H), 3.97 (s, 3H), 3.94 (s, 3H), 3.05-2.95 (m, 1H), 2.75-2.66 (m, 2H), 2.32-2.20 (m, 1H), 1.87 (t, *J* = 13.4 Hz, 2H), 1.50-1.34 (m, 1H), 1.40 (t, *J* = 7.1 Hz, 3H), 1.08 (d, *J* = 6.5 Hz, 3H). ^{13}C NMR (75 MHz, $CDCl_3$) δ 166.65, 162.71, 152.23, 148.92, 148.30, 130.65, 126.13, 124.89, 119.76, 111.17, 110.61, 110.22, 60.17, 55.72, 55.69, 34.49, 30.77, 28.62, 23.83, 21.39, 14.01. HRMS calculated for $C_{21}H_{25}NO_5S$ $(M+H)^+$: 404.1526, found: 404.1524.

2-(3-Cyclopentylpropanamido)-6-methyl-4,5,6,7-tetrahydro-benzo[*b*]thiophene-3-carboxylic acid propyl ester (**3**) was synthesized in line with the general procedure with compound **3a** (0.4 g, 1.6 mmol) and 3-cyclopentylpropanoyl chloride (0.283 g, 1.8 mmol). The crude product was purified with column chromatography on silica gel (Petroleumether ether/ethyl acetate = 30:1, v/v). White solid; yield 85.10%; mp: 60-61 □; ^{1}H NMR (300 MHz, $CDCl_3$) δ 11.28 (s, 1H), 4.23 (t, *J* = 6.5 Hz, 2H), 2.99-2.87 (m, 1H), 2.76-2.59 (m, 2H), 2.51-2.42 (m, 2H), 2.30-2.17 (m, 1H), 1.92-1.70 (m, 9H), 1.65-1.46 (m, 4H), 1.43-1.28 (m, 1H), 1.26-0.97 (m, 2H), 1.05 (d, *J* = 6.5 Hz, 3H), 1.02 (t, *J* = 7.4 Hz, 3H). ^{13}C NMR (75 MHz, $CDCl_3$) δ 169.20, 165.78, 146.94, 129.30, 125.22, 110.08, 65.15, 38.62, 35.24, 31.43, 30.49, 30.18, 28.24, 25.22, 24.14, 21.08, 20.36, 9.75. HRMS calculated for $C_{21}H_{31}NO_3S$ $(M+H)^+$: 378.2097, found: 378.2095.

6-(Tert-butyl)-2-(cyclopropanecarboxamido)-4,5,6,7-tetrahydro-benzo[*b*]thiophene-3-carboxylate

198 acid ethyl ester (**4**) was synthesized in line with the general procedure with compound **4a** (0.350 g,
199 1.2 mmol) and cyclopropanecarbonyl chloride (0.142 g, 1.4 mmol). The crude product was purified
200 with column chromatography on silica gel (Petroleumether ether/ethyl acetate = 250:9, v/v). White
201 solid; yield 87.23%; mp: 130-131 □; ^{1}H NMR (300 MHz, DMSO-d_6) δ 11.21 (s, 1H), 4.28 (q, J =
202 7.1 Hz, 2H), 3.02-2.88 (m, 1H), 2.67-2.39 (m, 2H), 2.38-2.22 (m, 1H), 2.03-1.87 (m, 2H), 1.46-1.36
203 (m, 1H), 1.32 (t, J = 7.1 Hz, 3H), 1.26-1.08 (m, 1H), 1.00-0.82 (m, 4H), 0.90 (s, 9H). ^{13}C NMR (75
204 MHz, DMSO-d_6) δ 170.42, 165.05, 146.48, 130.25, 126.41, 110.56, 60.25, 44.39, 32.11, 27.07, 26.93,
205 25.25, 23.99, 14.63, 8.32. HRMS calculated for $C_{19}H_{27}NO_3S$ $(M+H)^+$: 350.1784, found: 350.1779.

206 6-Methyl-2-(thiophene-2-carboxamido)-4,5,6,7-tetrahydro-benzo[*b*]thiophene-3-carboxylic acid
207 isopropyl ester (**5**) was synthesized in line with the general procedure with compound **5a** (0.8 g, 3.2
208 mmol) and thiophene-2-carbonyl chloride (0.695 g, 4.7 mmol). The crude product was purified with
209 column chromatography on silica gel (Petroleumether ether/ethyl acetate = 30:1, v/v). Yellow solid;
210 yield 85.64%; mp: 183-184 □; ^{1}H NMR (300 MHz, $CDCl_3$) δ 12.20 (s, 1H), 7.75 (d, J = 3.6 Hz, 1H),
211 7.58 (d, J = 4.9 Hz, 1H), 7.17-7.11 (m, 1H), 5.33-5.18 (m, 1H), 3.02-2.89 (m, 1H), 2.80-2.60 (m, 2H),
212 2.34-2.21 (m, 1H), 1.94-1.83 (m, 2H), 1.49-1.24 (m, 1H),1.38 (d, J = 10.1 Hz, 3H), 1.38 (d, J = 2.3
213 Hz, 3H), 1.07 (d, J = 6.5 Hz, 3H). ^{13}C NMR (75 MHz, $CDCl_3$) δ 166.53, 158.36, 147.69, 137.89,
214 131.75, 130.85, 129.31, 128.09, 126.90, 112.10, 68.36, 32.61, 31.24, 29.33, 26.38, 22.20, 22.17,
215 21.47. HRMS calculated for $C_{18}H_{21}NO_3S_2$ $(M+H)^+$: 364.1036, found: 364.1032.

216 2-(4-Chlorobutanamido)-6-methyl-4,5,6,7-tetrahydro-benzo[*b*]thiophene-3-carboxylate acid ethyl
217 ester (**6**) was synthesized in line with the general procedure with compound **1** (0.598 g, 2.5 mmol)
218 and 4-chlorobutanoyl chloride (0.389 g, 2.8 mmol). The crude product was purified with column

219 chromatography on silica gel (Petroleumether ether/ethyl acetate = 20:1, v/v). White solid; yield
220 88.83%; mp: 64-65 □; ^{1}H NMR (300 MHz, DMSO-d_6) δ 11.01 (s, 1H), 4.26 (q, J = 7.1 Hz, 2H),
221 3.69 (t, J = 6.6 Hz, 2H), 2.83 (d, J = 17.4 Hz, 1H), 2.65 (t, J = 7.3 Hz, 2H), 2.62-2.47 (m, 2H),
222 2.21-2.11 (m, 1H), 2.11-1.98 (m, 2H), 1.85-1.69 (m, 2H), 1.36-1.16 (m, 1H), 1.30 (t, J = 7.1 Hz, 3H),
223 0.99 (d, J = 6.4 Hz, 3H). ^{13}C NMR (75 MHz, DMSO-d_6) δ 168.90, 165.07, 146.19, 129.97, 125.57,
224 111.04, 60.30, 44.55, 39.60, 32.97, 31.75, 30.57, 28.71, 27.76, 25.62, 21.17, 14.07. HRMS calculated
225 for $C_{16}H_{22}ClNO_3S$ $(M+H)^+$: 344.1082, found: 344.1079.

226 **Protein Expression and Purification**. Chitinase *Of*ChtI was overexpressed and purified
227 according to the methods of Chen *et al.*[41] Briefly, the DNA segment of *Of*Cht□ was amplified by
228 PCR, then the products were ligated to pPIC9 (Invitrogen, Carlsbad, CA). The plasmid
229 pPIC9-*Of*ChtI was transformed into *Pichia pastoris* GS115 (Invitrogen, Carlsbad, CA) by
230 electroporation. *P. pastoris* cells expressing *Of*ChtI were grown in 100 ml of BMGY medium (1%
231 yeast extract, 2% peptone, 1% glycerol, 0.2% biotin, 1.34% yeast nitrogen, 10 ml of 100 mM
232 potassium phosphate, and 90 ml water, pH 6.0) at 30 □ for 24 h. Then the cells were resuspended in
233 500 ml of BMMY medium (1% yeast extract, 2% peptone, 1% methanol, 0.2% biotin, 1.34% yeast
234 nitrogen, 50 ml of 100 mM potassium phosphate, and 450 ml water, pH 6.0) at 30 □ for 72 h, and 5
235 ml methanol was added to the mixture every 24 hours as an inducer. After that, the supernatant was
236 obtained by centrifuging and placed in ammonium sulfate (70% saturation) precipitation at 4 □. The
237 precipitation was dissolved in buffer (20 mM sodium dihydrogen phosphate, 500 mM sodium
238 chloride, and 20 mM imidazole, pH 7.4), and then purified by metal-chelating chromatography with
239 a nickel-NTA-Sepharose high performance column, 5 ml (GE Healthcare, Shanghai, China). Finally,

240 the target protein was eluted in the buffer (20 mM sodium dihydrogen phosphate, 500 mM sodium
241 chloride, and 200 mM imidazole, pH 7.4) and then collected. The BCA protein assay kit (TaKaRa,
242 Dalian, China) was used to quantitate the protein and its purity was analyzed by SDS-PAGE.

243

244 **Enzymatic Assay.** Enzymatic activity was determined using
245 4-methylumbelliferyl-*N*,*N*'-diacetyl-β-D-chitobioside (Sigma, Shanghai, China) as substrate. The
246 reaction mixture used for inhibitor screening consisted of 100 μL of 30 μM of substrate, 10 nM
247 enzyme, 100 μM inhibitor, and 2% dimethylsulfoxide in a 20 mM sodium phosphate buffer (pH 6.0).
248 The reaction mixture without inhibitor was used as a positive control. After incubation at 30 □ for 20
249 min, 100 μL of 0.5 M Na_2CO_3 was added to the reaction mixture, and the fluorescence of the released
250 4-methylumbelliferone was quantitated by a microplate reader with excitation and emission
251 wavelengths of 360 and 450 nm, respectively. Experiments were performed in triplicate unless
252 specified otherwise. For K_i value determination, three substrate concentrations (1, 2 and 4 μM) and
253 varied inhibitor concentrations were used. The K_i values and types of inhibition were determined by
254 linear fitting of data in Dixon plots.

255

256 **RESULTS AND DISCUSSION**

257 **Compounds Obtained by Structure-based Virtual Screening.** It is reasonable to expect that the
258 constraints imposed by the physical properties of a molecule on its ability to express pesticide-like
259 activity are important in the selection of potential molecular candidates. The SPECS database

260 contains a large number of compounds whose properties are unlike those of pesticides. Therefore, in
261 order to limit the amount of time spent screening inappropriate molecules, established
262 pesticide-likeness rules[38] were used to filter out unsuitable compounds from the database. This led to
263 the formation of a reduced and refined dataset (dataset 1) which consisted of 72,720 small molecules.
264 This strategy effectively reduced the breadth of screening, and at the same time increasing the
265 chances of identifying suitable candidate molecules.

266 The dataset 1 was then screened by a well-established pharmacophore model. 3WL1 is the first
267 reported crystal structure of *Of*ChtI with two substrates $(GlcNAc)_2$ and $(GlcNAc)_3$ together. The
268 $(GlcNAc)_2$ takes up the binding subsites +1 and +2, while the $(GlcNAc)_3$ extends from the subsites
269 -1, to -3. 3WQV is the *Of*ChtI with inhibitor $(GlcN)_5$, and the ligand occupied the subsites -1 to -5.
270 Compared the two structures, they share the same binding subsites -1, -2 and -3, which are thought to
271 be more important in the binding process.[35] According to these considerations, the pharmacophore
272 model was firstly generated by the interactions between *Of*ChtI and $(GlcNAc)_3$. The key animo acids
273 Trp372, Glu148, Trp107, and Trp34 were used to create pharmacophore features. However, less than
274 1,000 molecules were filtered out by this model, due to too many feature restraints. Thus, this
275 pharmacophore model was not suitable for the present purpose. In order to optimize the
276 pharmacophore model, the crystal structures of 3WL1 and 3WQV were superposed, and three
277 common residues, Trp107, Glu148, Trp372 were found. So, these residues were used to refine a
278 pharmacophore model. Based on the modified model, 17,000 compounds were obtained and used to
279 formulate a new dataset: dataset 2.

280 Molecular docking was employed in order to generate elementary prediction of the binding modes

281 and affinities between the protein and the candidate inhibitors contained in the dataset 2. The
282 bioactive conformation of *Of*ChtI in complex with $(GlcNAc)_3$ was used as a template for the
283 molecular docking, and docking was accomplished at subsites -1 to -3 of *Of*ChtI, using MOE
284 modelling software. The obtained poses were rank-ordered according to their scores, which provided
285 the indication of accuracy and stability of the docking, the more negative the score, the more stable
286 the interaction. On that basis, for each compound the pose with the lowest score was retained, and
287 the top 20% of the resulting compounds, whose scores ranged from -8.76 to -6.96, were selected to
288 form dataset 3.

289 Cluster analysis of dataset 3 using the SAReport program resulted in 27 clusters with diverse
290 scaffolds. The largest cluster contained 225 compounds with a 4,5,6,7-tetrahydrobenzo[*b*]thiophene
291 chemical scaffold. Somewhat surprisingly, almost 16.1% of the dataset 3 was comprised of
292 molecules with this scaffold, while less than 1% of compounds in the entire SPECS database did so.
293 For this reason, this scaffold type was considered as a top priority for further investigations of *Of*ChtI
294 enzyme inhibitory activity. The utilization of cluster analysis to discover a common chemical
295 fragment markedly increased the efficiency of the screening process.

296 A fragment of 2-amino-6-methyl-4,5,6,7-tetrahydro-benzo[*b*]thiophene-3-carboxylic acid ethyl
297 ester, **1** (Figure 3) was selected and its *Of*ChtI inhibitory activity was cautiously assessed *via* a
298 bioassay. As predicted, it showed an inhibitory effect against *Of*ChtI, but the effect was relatively
299 weak (K_i = 26.3 μM) (Table 1). Nevertheless, the results verified that a new type of scaffold with
300 inhibitory activity had been identified. Furthermore, the fragment was observed to exhibit a variety
301 of structural forms comprising a number of different varied subunits. Five different compounds, **2-6**

302 (Figure 3) from the largest subunit were selected for chemical synthesis and used to test their
303 inhibitory activities against *Of*ChtI. The results showed that the inhibitory activities of four of these
304 compounds, **3**-**6** were largely improved, compared with the parent fragment **1**, and also better than
305 the control $(GlcN)_5$ (K_i = 15.2 μM). Especially compound **3**, which had excellent inhibitory effect (K_i
306 = 1.5 μM), while compounds **4**-**6** exhibited K_i values of 2.4 μM, 3.5 μM and 9.7 μM, respectively
307 (Table 1). And, they were determined to be competitive inhibitors against *Of*ChtI (Figure 4).
308 Strangely, the *Of*ChtI inhibitory effect of compound **2** decreased to 1.3% at 100 μM (Table 1).

309 Structural comparison of compounds **3**-**6** revealed that there were three major variants influencing
310 the inhibitory activity, at positions R_1, R_2 and R_3, respectively, but the differences between the
311 compounds were only minor (Figure 3). The primary difference between compound **2** and the other
312 compounds was the position of the R_1 group, which is the most likely reason for its lower inhibitory
313 activity. This will be further explored in our future research. It should be noted that the chemicals
314 required to synthesize the compounds are readily available and easy to obtain, and the synthetic route
315 of manufacture resulted in high atom economy with perfect utilization of reactant atoms in the end
316 product (Figure 1). Nevertheless, the novel scaffold identified herein warrants further exploration as
317 an inhibitor of *Of*ChtI. Whilst the inhibitory activities of the identified compounds are somewhat
318 limited, through efficient optimization it may well be possible to magnify their inhibitory effects
319 further.

320 **Structure-activity Relationship Analysis.** In order to obtain insights into the different *Of*ChtI
321 inhibition activities of the selected compounds **2**-**6**, their structure-activity relationships and
322 docking-predicted binding modes with the active sites of *Of*ChtI were analyzed carefully. The

323 chitinase *Of*ChtI is a monomer that contains a TIM-barrel catalytic domain which is composed of an
324 eight-stranded β-barrel surrounded by eight α-helices. It possesses a long cleft-like active pocket with
325 multiple binding subsites ranging from +2 to -5, these representing the non-reducing-end subsite and
326 reducing-end subsite, respectively. Among the selected compounds, compounds **3**-**6** exhibited strong
327 inhibition activities against *Of*ChtI, while compound **2** showed weak inhibition. Through analysis of
328 the predicted binding modes of these compounds it could readily be seen that the compounds **3**-**6**
329 exhibited the same binding modes with the ligand $(GlcNAc)_3$ in the active site. They all took up the
330 binding subsites from -1 to -3, and binding via hydrophobic and stacking interactions with certain
331 aromatic residues, including Trp372, Trp34, Trp107, Tyr272, Tyr30, Phe309, and Phe61 (Figure 5).
332 However, the predicted binding mode of compound **2** indicated a very poor substitution of the
333 5-methyl at R_1 position which could result in the entire compound far away from subsite -1 in the
334 active site than the other compounds because of the limited space available. Thus, in compound
335 **2**-*Of*ChtI, the stacking interactions with Trp372 could be destroyed. In fact, the rear end of the
336 *Of*ChtI active site was so large that it could easily accommodate a number of varied chemical groups
337 and big groups seemed to be useful, which might explain the observed differences in inhibition
338 effects of the compounds **3**-**6** and also provide a focus for future attempts to design inhibitors with
339 improved potency. Taken together, our findings suggest that the 5-group substitution at the R_1
340 position is not a useful target for improving the inhibitory activities of these compounds. However,
341 the stacking interactions with Trp372 and the hydrophobic interactions are indispensable, and the
342 space at the end of active site presents further opportunities for the future design of more potent
343 inhibitor compounds.

In the present study, we develop and employ a structure-based virtual screening methodology to identify a novel and potent scaffold against *Of*ChtI efficiently, which has the simpler structure than known inhibitors. Furthermore, the chemicals applied to the synthesis are easy to obtain. The synthetic route of compounds results in high atom economy with perfect utilization of reactant atoms in the end product. The inhibitory activities of four out of the five synthesized compounds (**3**-**6**) against *Of*ChtI were determined as relatively strong, and analysis of their structure-activity relationships provided insight into their interactions with the active site, which would inform future research to improve the potency of the inhibitory activity. This work presents a novel scaffold for inhibition of chitinases that warrants further exploitation and, in addition, offers an alternative approach for the application of virtual screening for pesticide identification more widely.

ABBREVIATIONS USED

GlcNAc, *N*-acetyl-D-glucosamine; GH18, glycoside hydrolase family 18; SBVS, structure-based virtual screening; GlcN, D-glucosamine; MW, molecular weight; Clog P, octanol-water partition coefficient; ROB, number of rotatable bonds; ARB, number of aromatic bonds; HBA, number of H-bond acceptors; HBD, number of H-bond donors;

ACKNOWLEDGEMENTS

This work was supported by the National Key R&D Program of China (No. 2017YFD0200504, 2017YFD0200501), and the National Natural Science Foundation of China (No. 21672257).

364

365 **SUPPORTING INFORMATION**

366 Predicted binding energies of the screened compounds; the initial pharmacophore model; K_i values of

367 compounds **4-6**, and $(GlcN)_5$ against *Of*ChtI; docking-predicted binding modes of compounds **1-6** in

368 the *Of*ChtI active site; ^{1}H NMR and ^{13}C NMR spectra of the compounds **1-6**, **2a-5a**.

369

370 **REFERENCES**

371 1. Neville, A. C.; Parry, D. A.; Woodhead-Galloway, J. The chitin crystallite in arthropod cuticle. *J.*
372 *Cell Sci.* **1976**, *21*, 73-82.

373 2. Zhu, K. Y.; Merzendorfer, H.; Zhang, W.; Zhang, J.; Muthukrishnan, S. Biosynthesis, turnover,
374 and functions of chitin in insects. *Annu. Rev. Entomol.* **2016**, *61*, 177-96.

375 3. Kramer, K. J.; Hopkins, T. L.; Schaefer, J. Applications of solids NMR to the analysis of insect
376 sclerotized structures. *Insect Biochem. Molec. Biol.* **1995**, *25*, 1067-1080.

377 4. Adrangi, S.; Faramarzi, M. A. From bacteria to human: a journey into the world of chitinases.
378 *Biotechnol. Adv.* **2013**, *31*, 1786-1795.

379 5. Genta, F. A.; Blanes, L.; Cristofoletti, P. T.; do Lago, C. L.; Terra, W. R.; Ferreira, C. Purification,
380 characterization and molecular cloning of the major chitinase from *Tenebrio molitor* larval midgut.
381 *Insect Biochem. Mol. Biol.* **2006**, *36*, 789-800.

382 6. Fukamizo, T.; Kramer, K. J. Mechanism of chitin oligosaccharide hydrolysis by the binary
383 enzyme chitinase system in insect moulting fluid. *Insect Biochem.* **1985**, *15*, 1-7.

384 7. Merzendorfer, H.; Zimoch, L. Chitin metabolism in insects: structure, function and regulation of
385 chitin synthases and chitinases. *J. Exp. Biol.* **2003**, *206*, 4393-4412.

386 8. Cohen, E. Chitin synthesis and degradation as targets for pesticide action. *Arch. Insect Biochem.*
387 *Physiol.* **1993**, *22*, 245-261.

388 9. Donnelly, L. E.; Barnes, P. J. Acidic mammalian chitinase - a potential target for asthma therapy.
389 *Trends Pharmacol. Sci.* **2004**, *25*, 509-511.

390 10. Hollak, C. E.; van Weely, S.; van Oers, M. H.; Aerts, J. M. Marked elevation of plasma

391 chitotriosidase activity. A novel hallmark of Gaucher disease. *J. Clin. Invest.* **1994**, *93*, 1288-1292.

392 11. Kramer, K. J.; Muthukrishnan, S. Insect chitinases: molecular biology and potential use as
393 biopesticides. *Insect Biochem. Molec. Biol.* **1997**, *27*, 887-900.

394 12. Pantoom, S.; Vetter, I. R.; Prinz, H.; Suginta, W. Potent family-18 chitinase inhibitors: X-ray
395 structures, affinities, and binding mechanisms. *J. Biol. Chem.* **2011**, *286*, 24312-24323.

396 13. Takeo, S.; Hisamori, D.; Matsuda, S.; Vinetz, J.; Sattabongkot, J.; Tsuboi, T. Enzymatic
397 characterization of the *Plasmodium vivax* chitinase, a potential malaria transmission-blocking target.
398 *Parasitol. Int.* **2009**, *58*, 243-248.

399 14. Nakanishi, E.; Okamoto, S.; Matsuura, H.; Nagasawa, H.; Sakuda, S. Allosamidin, a chitinase
400 inhibitor produced by *Streptomyces*, acts as an inducer of chitinase production in its producing strain.
401 *Proc. Japan Acad. Ser. B.* **2001**, *77*, 79-82.

402 15. Sakuda, S.; Isogai, A.; Matsumoto, S.; Suzuki, A. Search for microbial insect growth regulators.
403 II. Allosamidin, a novel insect chitinase inhibitor. *J. Antibiot. (Tokyo)* **1987**, *40*, 296-300.

404 16. Sakuda, S.; Isogai, A.; Makita, T.; Matsumoto, S.; Koseki, K.; Kodama, H.; Suzuki, A.
405 Structures of allosamidins, novel insect chitinase inhibitors, produced by *Actinomycetes*. *Agric. Biol.*
406 *Chem.* **1987**, *51*, 3251-3259.

407 17. Omura, S.; Aral, N.; Yamaguchi, Y.; Masuma, R.; Iwai, Y.; Namikoshi, M.; Turberg, A.; Kolbl,
408 H.; Shiomi, K. Argifin, a new chitinase inhibitors, produces by *Gliocladium* sp. FTD-0668. *J.*
409 *Antibiot.* **2000**, *53*, 603-608.

410 18. Arai, N.; Shiomi, K.; Yamaguchi, Y.; Masuma, R.; Iwai, Y.; Turberg, A.; Kolbl, H.; Omura, S.
411 Argadin, a new chitinase inhibitor, produced by *Clonostachys* sp. FO-7314. *Chem. Pharm. Bull.*

412 **2000**, *48*, 1442−1446.

413 19. Houston, D. R.; Eggleston, I.; Synstad, B.; Eijsink, V. G.; van Aalten, D. M. The cyclic dipeptide
414 CI-4[cyclo-(L-Arg-D-Pro)] inhibits family 18 chitinases by structural mimicry of a reaction
415 intermediate. *J. Biochem.* **2002**, *368*, 23-27.

416 20. Tabudravu, J. N.; Eijsink, V. G.; Gooday, G. W.; Jaspars, M.; Komander, D.; Legg, M.; Synstad,
417 B.; Van Aalten, D. M. Psammaplin A, a chitinase inhibitor isolated from the Fijian marine sponge
418 *Aplysinella Rhax*. *Bioorg. Med. Chem.* **2002**, *10*, 1123−1128.

419 21. Kato, T.; Shizuri, Y.; Izumida, H.; Yokoyama, A.; Endo, M. Styloguanidines, new chitinase
420 inhibitors from the marine sponge *Stylotella aurantium*. *Tetrahedron Lett*. **1995**, *36*, 2133-2136.

421 22. Chen, L.; Zhou, Y.; Qu, M.; Zhao, Y.; Yang, Q. Fully deacetylated chitooligosaccharides act as
422 efficient glycoside hydrolase family 18 chitinase inhibitors. *J. Biol. Chem.* **2014**, *289*, 17932-17940.

423 23. Rao, F. V.; Andersen, O. A.; Vora, K. A.; Demartino, J. A.; van Aalten, D. M. Methylxanthine
424 drugs are chitinase inhibitors: investigation of inhibition and binding modes. *Chem. Biol.* **2005**, *12*,
425 973-980.

426 24. Schuttelkopf, A. W.; Andersen, O. A.; Rao, F. V.; Allwood, M.; Lloyd, C.; Eggleston, I. M.; van
427 Aalten, D. M. Screening-based discovery and structural dissection of a novel family 18 chitinase
428 inhibitor. *J. Biol. Chem.* **2006**, *281*, 27278-27285.

429 25. Hao, G. F.; Wang, F.; Li, H.; Zhu, X. L.; Yang, W. C.; Huang, L. S.; Wu, J. W.; Berry, E. A.;
430 Yang, G. F. Computational discovery of picomolar Qo site inhibitors of cytochrome bc_1 complex. *J.*
431 *Am. Chem. Soc.* **2012**, *134*, 11168-11176.

432 26. Lai, X.; Wolkenhauer, O.; Vera, J. Understanding microRNA-mediated gene regulatory networks

433 through mathematical modelling. *Nucleic Acids Res.* **2016**, *44*, 6019-6035.

434 27. Xiong, L.; Li, H.; Jiang, L. N.; Ge, J. M.; Yang, W. C.; Zhu, X. L.; Yang, G. F. Structure-based
435 discovery of potential fungicides as succinate ubiquinone oxidoreductase inhibitors. *J. Agric. Food*
436 *Chem.* **2017**, *65*, 1021-1029.

437 28. Xiong, L.; Zhu, X. L.; Gao, H. W.; Fu, Y.; Hu, S. Q.; Jiang, L. N.; Yang, W. C.; Yang, G. F.
438 Discovery of potent succinate-ubiquinone oxidoreductase inhibitors via pharmacophore-linked
439 fragment virtual screening approach. *J. Agric. Food Chem.* **2016**, *64*, 4830-4837.

440 29. Cole, D. C.; Olland, A. M.; Jacob, J.; Brooks, J.; Bursavich, M. G.; Czerwinski, R.; Declercq, C.;
441 Johnson, M.; Joseph-McCarthy, D.; Ellingboe, J. W.; Lin, L.; Nowak, P.; Presman, E.; Strand, J.; Tam,
442 A.; Williams, C. M.; Yao, S.; Tsao, D. H.; Fitz, L. J. Identification and characterization of acidic
443 mammalian chitinase inhibitors. *J. Med. Chem.* **2010**, *53*, 6122-6128.

444 30. Jiang, X.; Kumar, A.; Liu, T.; Zhang, K. Y.; Yang, Q. A novel scaffold for developing specific or
445 broad-spectrum chitinase inhibitors. *J. Chem. Inf. Model.* **2016**, *56*, 2413-2420.

446 31. Chu, H.; Wang, J.; Shen, H.; Yang, y.; Zhu W.; Li, G. Investigation of family 18 chitinases and
447 inhibitors by computer-aided approaches. *Curr. Drug Targets.* **2012**, *13*, 502-511.

448 32. Vaaje-Kolstad, G.; Horn, S. J.; Sorlie, M.; Eijsink, V. G. The chitinolytic machinery of *Serratia*
449 *marcescens* - a model system for enzymatic degradation of recalcitrant polysaccharides. *FEBS J.*
450 **2013**, *280*, 3028-3049.

451 33. Liu, T.; Chen, L.; Ma, Q.; Shen, X.; Yang, Q. Structural insights into chitinolytic enzymes and
452 inhibition mechanisms of selective inhibitors. *Curr. Pharm. Design* **2014**, *20*, 754-770.

453 34. Chen, L.; Liu, T.; Duan, Y.; Lu, X.; Yang, Q. Microbial secondary metabolite, phlegmacin B_1, as

454 a novel inhibitor of insect chitinolytic enzymes. *J. Agric. Food Chem.* **2017**, *65*, 3851-3857.

455 35. Chen, L.; Liu, T.; Zhou, Y.; Chen, Q.; Shen, X.; Yang, Q. Structural characteristics of an insect
456 group I chitinase, an enzyme indispensable to moulting. *Acta Crystallogr D.* **2014**, *70*, 932-942.

457 36. SPECS: chemistry solutions for drug discovery. http://www.specs.net. (Accessed: October 1,
458 2011).

459 37. Molecular Operating Environment (MOE), 2016.08; Chemical Computing Group Inc., 1010
460 Sherbrooke St. West, Suite #910, Montreal, QC, Canada, H3A 2R7, 2016.

461 38. Hao, G.; Dong, Q.; Yang, G. A comparative study on the constitutive properties of marketed
462 pesticides. *Mol. Inf.* **2011**, *30*, 614-622.

463 39. Labute, P. The generalized born/volume integral implicit solvent model: estimation of the free
464 energy of hydration using London dispersion instead of atomic surface area. *J. Comput. Chem.* **2008**,
465 *29*, 1693-1698.

466 40. Clark, A. M.; Labute P. Detection and assignment of common scaffolds in project databases of
467 lead molecules. *J. Med. Chem.* **2009**, *52*, 469–483.

468 41. Wu, Q.; Liu, T.; Yang, Q. Cloning, expression and biocharacterization of *Of*Cht5, the chitinase
469 from the insect *Ostrinia furnacalis*. *Insect Sci.* **2013**, *20*, 147-157.

470

471 **FIGURE CAPTIONS:**

472 **Figure 1.** Synthetic route for preparation of compounds **2-6** and their precursors **2a-5a** and **1**.

473 Reagents and conditions: □ EtOH, morpholine, reflux, 5 h; □ CH_2Cl_2, TEA, r.t., overnight.

474

475 **Figure 2.** The final pharmacophore model used in the screening of *Of*ChtI inhibitors. Don|Acc:

476 hydrogen bond donor or acceptor. Don2|Acc2: projection of the donor or the acceptor. Hyd:

477 hydrophobic centroid.

478

479 **Figure 3.** Structures of compounds **1-6** identified by structure-based virtual screening.

480

481 **Figure 4.** Inhibitory kinetics of compounds **1** (A) and **3** (B) against *Of*ChtI.

482

483 **Figure 5.** A, Docking-predicted binding modes of compounds $(GlcNAc)_3$ (red), **3** (green), **4** (blue), **5**

484 (orange), **6** (carmine) in the *Of*ChtI active site. B, Docking-predicted binding mode of compound **3** in

485 the *Of*ChtI active site.

486

Table:

Table 1. Inhibitory Activities of Compounds **1-6** against *Of*ChtI.

Compounds	Inhibition Rate (%) (mean ± SD)		K_i (μM)
	100 μM	20 μM	
1	54.1 ± 3.1	24.8 ± 4.9	26.3
2	1.3 ± 3.4	0	ND[a]
3	99.0 ± 0.1	95.1 ± 1.2	1.5
4	95.2 ± 0.5	68.4 ± 5.9	2.4
5	100 ± 3.4	62.1 ± 2.2	3.5
6	96.2 ± 0.3	52.9 ± 4.0	9.7
$(GlcN)_5$[b]	75.6 ± 0.2	45.9 ± 0.4	15.2

[a] Not determined. [b] Control compound.

Figure Graphics:

Figure 1

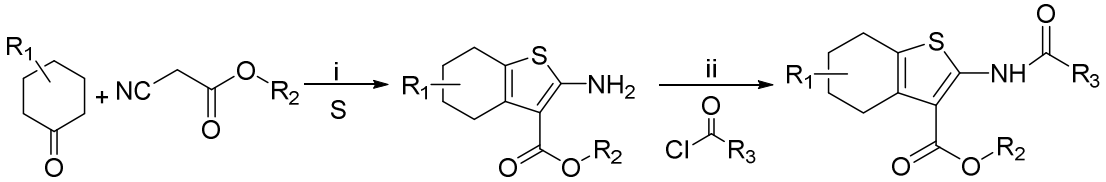

2a-5a,1 **2-6**

	2a/2	**3a/3**	**4a/4**	**5a/5**	**1/6**
R_1	5-CH_3	6-CH_3	6-$C(CH_3)_3$	6-CH_3	6-CH_3
R_2	-CH_2CH_3	-$CH_2CH_2CH_3$	-CH_2CH_3	-$CH(CH_3)_2$	-CH_2CH_3
R_3	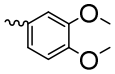	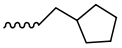			-$(CH_2)_3Cl$

Figure 2

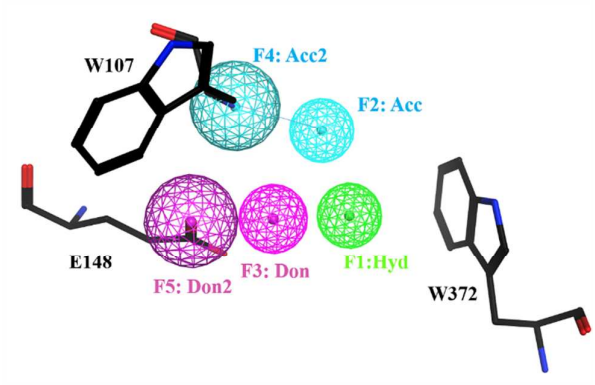

Figure 3

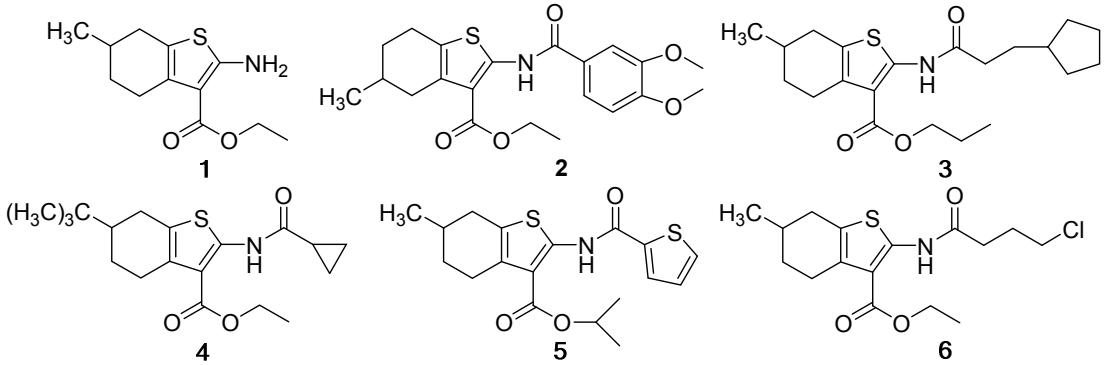

Figure 4

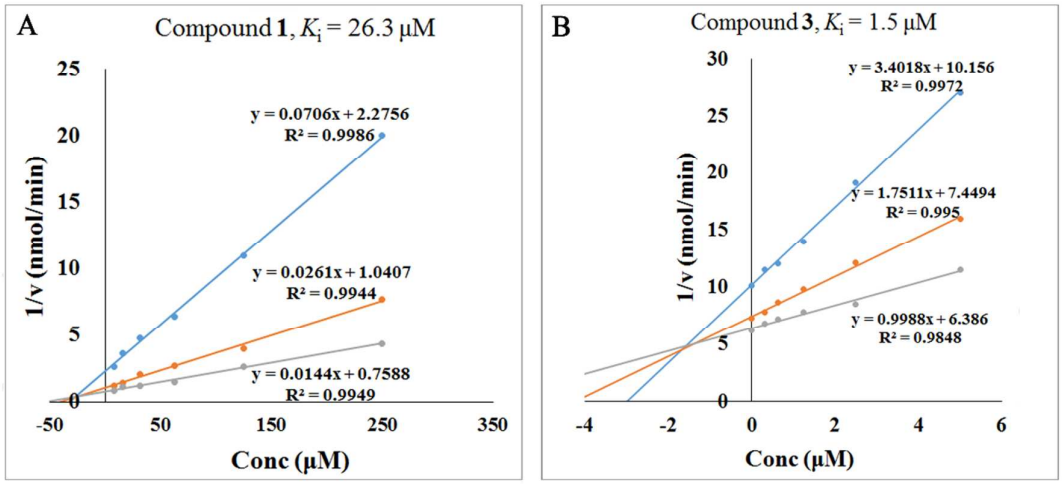
A
Compound 1, K_i = 26.3 μM
y = 0.0706x + 2.2756
R² = 0.9986
y = 0.0261x + 1.0407
R² = 0.9944
y = 0.0144x + 0.7588
R² = 0.9949
1/v (nmol/min)
Conc (μM)
B
Compound 3, K_i = 1.5 μM
y = 3.4018x + 10.156
R² = 0.9972
y = 1.7511x + 7.4494
R² = 0.995
y = 0.9988x + 6.386
R² = 0.9848
1/v (nmol/min)
Conc (μM)

Figure 5

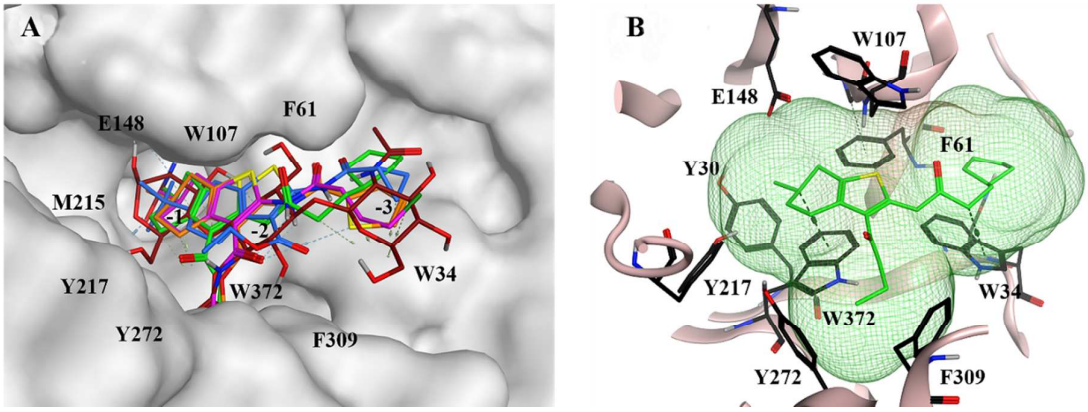
A
E148
W107
F61
M215
-1
-2
-3
W34
Y217
W372
Y272
F309
B
W107
E148
F61
Y30
Y217
W372
W34
Y272
F309

Table of Contents Graphic